Satellite Image Classification Using Expert Structural Knowledge: A Method Based on Fuzzy Partition Computation and Simulated Annealing

Hirotaka SUZUKI [1], Pascal MATSAKIS [2], Serge ANDRÉFOUËT [3], Jacky DESACHY [4]

[1] Université Paul Sabatier, Institut de Recherche en Informatique de Toulouse (IRIT)
118 route de Narbonne, 31062 Toulouse Cedex, France
Hirotaka.Suzuki@irit.fr

[2] University of Missouri-Columbia, Department of Computer Engineering and Computer Science
201 Engineering Building West, Columbia, MO 65211, USA
pmatsakis@cecs.missouri.edu

[3] University of South Florida, College of Marine Science, Remote Sensing and Biological Oceanography
140, 7th Av. South , St Petersburg, FL 33701, USA
serge@carbon.marine.usf.edu

[4] Université des Antilles et de la Guyane, UFR Sciences Exactes et Naturelles
Campus de Fouillole, 97159 Pointe à Pitre, Guadeloupe, France
Jacky.Desachy@univ-ag.fr

Abstract
The design of automatic systems dedicated to satellite image classification has received considerable attention. However, the current systems still cannot compare with human photo-interpreters. A promising approach consists in integrating structural knowledge into the classification process, i.e., using information about the shape of and the spatial relations between the regions that are to be determined. The present work tackles this issue, and relies on soft computing techniques. First, a fuzzy classifier produces a fuzzy partition of the image. Then, the defuzzified (crisp) partition is tried to be improved. According to the membership degrees in the fuzzy partition, the system selects a set of pixels and associates a set of candidate classes with each of them. The initial crisp partition is improved by reassigning each selected pixel to one of the classes it may belong to. This is performed by a combinatorial optimization strategy. The aim is to maximize the adequacy between the regions defined by the crisp partition and the structural knowledge which is available. First experiments on remote sensing data show the applicability of our approach.

Keywords
Remote sensing images, fuzzy classification,
expert structural knowledge, rule-based fuzzy systems, simulated annealing.

1. Introduction

The design of automatic systems dedicated to satellite image classification has received considerable attention. Although important results have been achieved, the current systems still cannot compare with human photo-interpreters. Numerous classifiers based on the spectral analysis of individual pixels have been proposed. However, the limitations when only using spectral information are apparent, and in most cases the classification results are unsatisfactory.

With the aim of achieving higher accuracy, integration of additional data has been investigated. The multisource classification model is based on pixel-by-pixel classification techniques that combine spectral information with various forms of data related to individual pixels (e.g., multisensor data, multitemporal data, ancillary data like

digital elevation models, geological and topographic maps, symbolic data such as model-based knowledge represented by if-then rules, etc.) [1][2][3]. The data obtained from different sources is generally described by different models and contains uncertain and incomplete information. Therefore, data fusion methods relying on Dempster-Shafer's theory [4] and fuzzy set theory [5] have been successfully employed [6][7][8]. However, as expressed by the contextual classification model, each pixel should not be classified independently from its neighboring pixels [9]. Relaxation methods [10] and smoothing methods (sometimes referred to as generalization) [11] are representative of this concept. Finally, it is natural to utilize both the multisource and the contextual models to achieve higher classification accuracy [12][13].

Nevertheless, human photo-interpreters also implicitly use *structural* knowledge in the manual classification process. They not only consider contextual information but also information about the shape of and the spatial relations between the image regions. This type of knowledge has not been utilized in former systems. Several studies have exploited structural knowledge for classifying image segments produced by spectral image segmentation. The classes are described by knowledge-based rules, and each segment is classified according to its geometric and morphological properties [14]. But the results totally depend on the segmentation stage, which does not consider structural knowledge.

In this paper, we present an approach that integrates structural knowledge into the image classification process. First, a fuzzy classifier generates a fuzzy partition of the image. The partition can be either probabilistic or possibilistic. Its defuzzification produces a traditional crisp partition. The system then selects certain pixels, and a set of candidate classes is associated with each selected pixel. The pixels and classes are chosen according to the membership degrees in the fuzzy partition. Finally, the system tries to improve the initial classification by reassigning each pixel to one of the classes it may belong to. For these reassignments, it is assumed that some structural knowledge about the classes to be found in the image has been collected. We are faced with three fundamental problems: (1) How to represent the expert knowledge? (2) How to measure the adequacy between an image region and the knowledge that is supposed to concern it? (3) How to exploit such a measurement in the classification process? The first two problems are discussed briefly in Section 2. Our main interest is in the third problem. In Section 3, we describe a Region Modification Approach (RMA) by Simulated Annealing (SA). In Section 4, we present first experiments on remote sensing data: a Landsat 7 multispectral image of Tikehau atoll in French Polynesia. Conclusions and further comments are given in Section 5.

2. Knowledge Representation

Expert knowledge contains uncertain, incomplete and vague information. Consequently, the use of a fuzzy inference system appears to be justified. Fuzzy production rules for image classification are typically of the following form (although the premise and consequent could sometimes be reversed) [3][6][13]:

$$\text{If (class } k \text{), then (} V_1 \text{ is } A_1 \text{) and ... and (} V_i \text{ is } A_i \text{) and ... and (} V_N \text{ is } A_N \text{).}$$

The consequent term characterizes the environmental context of the class. It is composed of elementary propositions such as "V_i is A_i", where V_i denotes a variable and A_i a fuzzy subset. These propositions are connected by logical ANDs (ORs are also admitted). Generally A_i's are defined *a priori*, by interviewing experts, or *a posteriori*, using experimental methods [15].

2.1. Pixel-Related Knowledge

When the V_i 's are related to pixels (i.e., when each pixel can be considered independently of the others), the production rule represents "*pixel-related knowledge*". This knowledge may use pixel-related features (spectral data, altitude, etc.). This type of knowledge has already been studied [6].

2.2. Structural Knowledge

Now, consider the following expert knowledge: "class 1 appears principally in the shape of little circular regions". At this point, the pixels can no longer be classified independently from the others. This type of knowledge is called *structural knowledge*. In the example above, there are two elemental knowledge terms, "circular region" and "little region", which implicitly involve specific features (e.g., aspect ratio, area, etc.). In this paper, we assume that we know how to relate an appropriate set of variables to all of the elemental structural knowledge, and further, how to measure these variables, whether the considered region in the image is crisp or fuzzy (see, e.g., [16]). To

represent structural knowledge and to measure its adequacy with image objects, a multisource fuzzy inference system can be used [2][12][13]. For example, in the framework of hierarchical fuzzy production rules, the structural knowledge SK_k about the class k is represented as follows:

Upper level rule: If (class k), then (ESK_1) and ... and (ESK_j) and ... and (ESK_N).
Lower level rule: If (ESK_j), then (V_1^j is A_1^j) and ... and (V_i^j is A_i^j) and ... and ($V_{M_j}^j$ is $A_{M_j}^j$)

The consequent term of the upper level rule is composed of elemental knowledge terms ESK_j connected by logical ANDs (ORs are also admitted). In the lower level rule, each ESK_j is represented by measurable variables V_i^j and fuzzy subsets A_i^j. Note that the V_i^j are not concerned with pixels but with regions. Consider a region R that may be assigned to class k. The membership degree in A_i^j of the value V_i^j obtained at R corresponds to the degree of truth $\mu_{A_i^j}(R)$ of the proposition "V_i^j is A_i^j". The logical combination of the $\mu_{A_i^j}(R)$ gives $q^{ESK_j}(R)$, which is the degree of adequacy between the region R and the elemental structural knowledge ESK_j. Finally, at the upper level, the logical combination of the $q^{ESK_j}(R)$ gives $q^{SK_k}(R)$, the degree of adequacy between R and SK_k. Consider, for instance, the knowledge SK_2: "If (class 2), then (ESK_1) and (ESK_2)", where the lower level rules are "If (ESK_1), then (V_1^1 is A_1^1) or (V_2^1 is A_2^1)" and "If (ESK_2), then (V_1^2 is A_1^2)". We get:

$$q^{SK_2}(R) = \min\{\max\{\ \mu_{A_1^1}(R), \mu_{A_2^1}(R)\ \}, \mu_{A_1^2}(R)\ \}.$$

Note that Binaghi *et al*. [13] use a similar system to represent contextual information (in the upper level) and to evaluate multisource information (in the lower level). Also note that, in this paper, we do not describe how to handle adverbs (such as "principally") in the formulation of knowledge.

3. Structural Knowledge Integration

Suppose we are able to evaluate the degree of adequacy between any region and the structural knowledge that is available (Section 2). How can we utilize this ability to improve classification accuracy? We refer to this problem as the problem of *structural knowledge integration*. To answer it, we propose the Region Modification Approach.

3.1. Region Modification Approach (RMA)

Assume that a partition of the studied image has been output by some fuzzy classifier. We call this preliminary process *pre-classification*. The partition can be either probabilistic (the sum of the membership degrees is equal to 1) or possibilistic (the previous equality does not necessarily hold). Its defuzzification produces a traditional crisp partition. At first glance, by looking at this crisp partition, a human photo-interpreter may question the "class k" label assigned to a given region R, simply because R does not obviously conform to "class k" structural knowledge. The label might have been assigned by mistake (for instance, R is a region of "class m" whose spectral features resemble those of "class k"), or some boundary pixels (particularly mixed pixels) might have been misclassified. The human photo-interpreter will then revise the pre-classification output and reassign some pixels to other classes. The *Region Modification Approach* (RMA) imitates this process. Consider Fig. 1(a). It represents the crisp partition issued from some pre-classification. The black pixels are assigned to "class 1" and form the region R_1.

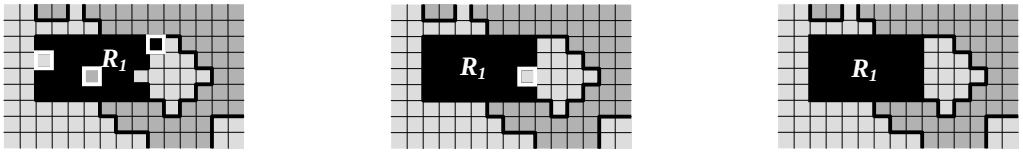

(a) $q^{SK1}(R_1)$ is low (b) $q^{SK1}(R_1)$ is high (c) $q^{SK1}(R_1)$ is maximum

Fig. 1. Is the region R_1 rectangular?

Suppose now that we have the structural knowledge SK_1: "class 1 appears in the shape of rectangular regions". It is obvious that the reassignment of some pixels (marked with white bordered squares) enables a significant increase of $q^{SK_1}(R_1)$, the degree of adequacy between R_1 and SK_1 (Fig. 1(b)(c)). Of course, if structural knowledge about the other classes is also available, this reassignment may simultaneously cause the decrease of adequacy degrees for neighboring regions. This is why we should consider a *global adequacy degree* $Q(X)$, the degree of adequacy between the partition and all the structural knowledge that is available. We have: $Q(X) = F(q_1, ..., q_r, ..., q_n)$, where X denotes the considered partition, F a combination operator, q_r the adequacy degree associated with the r-th region, and n the total number of regions in X. In our experiment (Section 4), the classical arithmetic mean operator has been chosen, but other operators (e.g., min operator) may also be considered.

The objective of the RMA is to reassign some pixels in order to globally increase the adequacy degrees of the regions. The problem corresponds to a combinatorial optimization problem. It aims at finding an optimal reassignment of pixels, i.e., a partition X that maximizes $Q(X)$. Three heuristic iterative methods are well known as efficient methods for answering optimization problems and have been successfully applied to clustering and image classification [17][18][19]: Simulated Annealing (SA), Tabu Search (TS), and Genetic Algorithm (GA). Their performances depend on the context of the problem (size and structure of search space, complexity of neighbor structure, etc.). In a previous study [20], we tested the RMA on a simple test image, and compared the use of the three heuristic methods. SA seemed to be the most appropriate. In this paper, we present the RMA by SA.

3.2. Simulated Annealing Strategy

The SA algorithm can be schematically described as follows: (I) From the current solution X^{now}, produce an alternative candidate solution X^{cand}. (II) If $Q(X^{now}) < Q(X^{cand})$, replace X^{now} by X^{cand}. (III) Repeat (I) and (II) until there are no solutions X^{cand} satisfying $Q(X^{now}) < Q(X^{cand})$. Unfortunately, the output of this algorithm may not be an optimal solution (local maximum only). This is why destructive solutions should sometimes be accepted, i.e., candidate solutions X^{cand} that do not satisfy the inequality $Q(X^{now}) < Q(X^{cand})$. In SA, this concept is implemented by introducing a parameter called temperature, and a cooling schedule.

In fact, the RMA requires a fuzzy pre-classification process. The initial solution X^{init} utilized in the RMA is a crisp partition obtained by defuzzifying the fuzzy partition $\tilde{X}$ issued from the pre-classification. Then, from a partition X^{now} (current solution), which is equal to X^{init} at the first iteration, an alternative partition X^{cand} is generated (in this paper, unless otherwise stated, the term "partition" always denotes a crisp partition). For any pixel P and any class i, let $\mu_i(P)$ be the membership value of P to class i in $\tilde{X}$, $CL^{init}(P)$ the class of P in X^{init}, and $CL^{now}(P)$ the class of P in X^{now}. For any i, $\mu_{CL^{init}(P)}(P) \geq \mu_i(P)$ is satisfied. The alternative partition X^{cand} is generated from X^{now} by reassigning a pixel P (chosen randomly) to a class $CL^{cand}(P) \neq CL^{now}(P)$ (chosen randomly too). However, it is obvious that a pixel P satisfying $\mu_{CL^{init}(P)}(P) >> \mu_i(P)$ for any $i \neq CL^{init}(P)$ would not constitute a judicious choice. Similarly, $CL^{cand}(P)$ should not satisfy $\mu_{CL^{init}(P)}(P) >> \mu_{CL^{cand}(P)}(P)$. Finally, X^{cand} is generated as follows:

[Step 1] Randomly choose a pixel P that satisfies
$min_{i \neq CL^{init}(P)}\{\mu_{CL^{init}(P)}(P) - \mu_i(P)\} \leq \sigma$
(where $\sigma \in [0,1]$ designates a predefined threshold).

[Step 2] Randomly choose a class $CL^{cand}(P)$ that satisfies
$\mu_{CL^{init}(P)}(P) - \mu_{CL^{cand}(P)}(P) \leq \sigma$.
If $CL^{cand}(P) = CL^{now}(P)$, return to Step 1.

[Step 3] Reassign P to class $CL^{cand}(P)$. The obtained partition is X^{cand}.

However, we can further refine the process. "Random" choices can be restrained so that *(i)* the lower $min_{i \neq CL^{init}(P)}\{\mu_{CL^{init}(P)}(P) - \mu_i(P)\}$, the higher the probability of choosing P, and *(ii)* the lower $\mu_{CL^{init}(P)}(P) - \mu_{CL^{cand}(P)}(P)$, the higher the probability of choosing $CL^{cand}(P)$. For instance, Step 2 can be rewritten as follows:

[Step 2] Select $CL^{cand}(P)$ by roulette selection: the probability of assigning P to a given class k is set to $\mu_k(P) / \Sigma_i \mu^*_i(P)$, where $\mu^*_i(P)$ equals $\mu_i(P)$ if $\mu_{CL^{init}(P)}(P) - \mu_i(P) \leq \sigma$ and equals 0 otherwise. If $CL^{cand}(P) = CL^{now}(P)$, return to Step 1.

Note that the fuzzy pre-classification may give a possibilistic partition [21]. In that case, $\Sigma_i \mu^*_i(P)$ is not necessarily equal to 1, even if σ=1. Also note that the output X^{init} of a crisp pre-classification can be used to produce a fuzzy partition. Let P be a pixel, and let R be a region assigned to class k in X^{init}. If P belongs to R, we can give $\mu_k(P)$ a value directly proportional to the distance of P from the boundary of R. Otherwise, we can give $\mu_k(P)$ a value inversely proportional to the distance of P from all regions assigned to class k. Then, the RMA would tend to round the regions which are expected to be round, to elongate those which are expected to be elongated, etc. The detailed algorithm is given below:

Initialization:
Set the iteration counter t to 1. Select a value for *it_max* (maximum number of iterations for **loop 2**), *IT_max* (maximum number of iterations for **loop 1**), and T_0 (initial temperature). Select a cooling schedule $\alpha(T)$ (in our experiments, we use $\alpha(T) = T_0 / t$). Initialize $X^{now} \leftarrow X^{init}$, where X^{init} denotes the partition issued from the pre-classification, and calculate $Q(X^{now})$.

Iteration loop 1
  Iteration loop 2
    1. Using X^{now}, generate a candidate partition X^{cand}.
    2. Calculate $\delta = Q(X^{now}) - Q(X^{cand})$. If $\delta < 0$, replace X^{now} by X^{cand}.
      Otherwise, select a random number $r \in [0,1]$, and if $r < \exp(\delta / T)$, replace X^{now} by X^{cand}.
  Repeat **loop 2** *it_max* times,
  Update $t \leftarrow t + 1$ and $T \leftarrow \alpha(T)$.
Repeat **loop 1** until t exceeds *IT_max* or Q reaches a predefined value. X^{now} is the final partition.

---

4. Experiments

4.1. Data and Pre-Classification Algorithm

In [23], we tested our approach on a 1D synthetic image and on a RGB image of a knife. In the present paper, for our first experiments on remote sensing data, we use a Landsat 7 multispectral image of Tikehau atoll in French Polynesia. The image was acquired on the 7th of August 1999. We exploit the first five bands (visible and infra-red) of the Enhanced Thematic Mapper Plus (ETM+) sensor onboard the Landsat 7 satellite. For each band, the spatial resolution is 30 meters. The images in Figures 2 and 3(a)(b) are obtained by attaching Red, Green and Blue values to the 4th, 2nd and 1st channels respectively.

The classifier that produces the fuzzy partition we need is a supervised fuzzy classifier. It derives from the unsupervised FCM (Fuzzy C-Means) [24] algorithm proposed by Gath and Geva [25]. It uses the Mahalanobis distance, and requires that each class be previously characterized by a prototype made of a mean vector and a covariance matrix. Fig. 3(c) shows the set of training pixels. The fuzzy partition is into 8 classes. These classes describe the morphology of a typical atoll rim of the Pacific Ocean (Fig. 2(b)(c)). Fig. 3(d) and Fig. 4(a) show the crisp partition attached to the fuzzy partition (i.e., obtained by "defuzzification").

Because they are both situated in a submerged domain of the atoll rim (shallow depth structures of the rim), the classes “spillway” and “reef flat” (classes 4 and 5) constitute one of the most important sources of misclassification. In general, their spectral characteristics are very similar, and they cannot be distinguished one from the other by conventional classifiers which utilize only spectral information and pixel-related knowledge [26][27]. For instance, in Fig. 4(b)(c), the next highest membership degree of most of the pixels assigned to “spillway” is the membership degree in class “reef flat”, and vice versa. The fundamental differences between the two classes are in their orientations—transversal for “spillway”, parallel to the coast line for “reef flat” (Fig. 2(b)(c))—and locations—“spillway” is generally located before “reef flat” in the transversal direction from the lagoon to the ocean. Reef flats do not link ocean and lagoon. They may be encountered even in closed atolls, along the oceanic side of the rim. Conversely, spillways work as a link between the ocean and the lagoon. Their role is critical for the renewal rate of lagoonal waters and the water quality inside lagoons [28]. Consequently, estimation of water renewal rate requires a clear discrimination and accurate quantification of the extent of spillways and reef flats along the atoll rim. For obtaining a high accuracy, consideration of geomorphological expertise is indispensable.

4.2. Expert Structural Knowledge

Knowledge 1
According to experts, along any cross section of the atoll rim, from the lagoon to the ocean, the geomorphological classes are situated not in random order, but in the following specific order:

"lagoon" ⇒ ("intertidal") ⇒ (("rubble") ⇒ ("vegetation") ⇒ "rubble" ⇒ ("intertidal")) ⇒ ("spillway")
⇒ ("intertidal") ⇒ "reef flat"/ "intertidal" ⇒ ("intertidal") ⇒ ("breaking wave") ⇒ "outer slope",

where ( ) means facultative appearance and / means alternative appearance.

Knowledge 2
In addition to *Knowledge 1*, in order to distinguish between "spillway" and "reef flat", experts implicitly carry out the following alternative reasoning:

1) Pick out a region that is potentially classifiable into "spillway" or "reef flat".
2) Generate a section parallel to the coast line (about 1 km long) and a cross section that both pass through the chosen region.
3) A. If the parallel section includes "rubble" or "vegetation", then the region is "spillway".
   B. Otherwise, if the sequence along the cross section (cf. *Knowledge 1*) includes "rubble" or "vegetation", then the region is "reef flat". Otherwise, the region is "spillway".

4.3. Knowledge Representation and Adequacy Degrees

In this paper, we simplify the classification problem described above by considering cross sections of the atoll rim and performing the RMA on "one-dimensional" partitions. Fifteen representative cross sections were selected (Fig. 4(a)). To each section corresponds a one-dimensional fuzzy partition (Fig. 4(b)(c)), and a one-dimensional crisp partition P (obtained by defuzzification). P is composed of a certain number of regions (segments). For each region R assigned to "spillway" or "reef flat", two state flags *p_flag(R)* and *v_flag(R)* are defined:

1) If P contains "rubble" or "vegetation", *p_flag(R)* is set *true.* Otherwise, *p_flag(R)* is set *false*.
2) If any parallel section passing through R contains "rubble" or "vegetation", *v_flag(R)* is set *true.* Otherwise, *v_flag(R)* is set *false*.

Knowledge 1 and *Knowledge 2* can be represented by the following If-Then production rules:

1) If ("spillway"), then (***ESK1***: "*R* conforms to the order in *Knowledge 1*")
   and (***ESK2***: "*v_flag(R)* is *true*" or ("*v_flag(R)* is *false*" and "*p_flag(R)* is *false*")).
2) If ("reef flat"), then (*ESK1*: "*R* conforms to the order in *Knowledge 1*")
   and (***ESK3***: "*v_flag(R)* is *false*" and "*p_flag(R)* is *true*").
3) If (not "spillway" and not "reef flat"), then (*ESK1*: "*R* conforms to the order in *Knowledge 1*").

The computation of $q^{ESK1}(R)$, the degree of adequacy between R and *Knowledge 1*, raises a *Sequence Comparison Problem* [29]. First, from the rule that represents *Knowledge 1*, the set $S=\{s_1, \ldots, s_{512}\}$ of all possible sequences (there are 512 possible sequences), is produced. For instance, the following sequence belongs to S:

"lagoon" ⇒ "spillway" ⇒ "intertidal" ⇒ "reef flat" ⇒ "breaking wave" ⇒ "outer slope".

Then $q^{ESK1}(R)$ is calculated by using the Levenshtein distance [30], which is one of the most popular criteria for evaluating a resemblance (similarity) between two words (sequences). Let P^* be the sequence of classes in P. For instance, if P = [1,1,1,2,2,3,1,1] (8 pixels, from the lagoon to the ocean), then P^* = [1,2,3,1]. For each possible order $s_j \in S$, the Levenshtein distance $d(P^*, s_j)$ between P^* and s_j is calculated. The distance $d(P^*, S)$ between P^* and S is given by: $d(P^*, S) = \min\{d(P^*, s_1), \ldots, d(P^*, s_{512})\}$. If $d(P^*, S)$ is zero, P^* corresponds to one sequence in S. The value $q^{ESK1}(R)$ is obtained by normalizing $d(P^*, S)$: $q^{ESK1}(R) = \max\{0, 1-d(P^*, S) / 20\}$. Note that this value only depends on P.

To compute $q^{ESK2}(R)$, we simply add a penalty distance to $d(P^*, S)$: $q^{ESK2}(R) = \max\{0,1-(d(P^*,S)+PD_2(R))/20\}$. If the binary condition attached to *ESK2* is *true*, the penalty distance $PD_2(R)$ is 0. Otherwise, $PD_2(R)$ is the number of pixels of R. The same applies to *ESK3*. Finally, the degree of adequacy between R and the expert knowledge is calculated as follows:

$q(R) = q^{ESK1}(R)$, when R is neither "spillway" nor "reef flat",
$q(R) = \min\{q^{ESK1}(R), q^{ESK2}(R)\}$, when R is "spillway",
$q(R) = \min\{q^{ESK1}(R), q^{ESK3}(R)\}$, when R is "reef flat",

and the global adequacy degree of P is $Q(P) = F(q(R_1), \ldots, q(R_n))$, where n is the total number of regions R_i in P, and $F(\,)$ is the arithmetic mean operator.

4.4. Selecting Parameter Values

Because the choice of values for T_0 and *it_max* is critical (Section 3.2), we first processed a test section (Fig. 4(a)) with different pairs of values for these parameters. For each pair, RMA was executed 10 times, and the average CPU time required for reaching $Q(P)>0.9$ was computed. Any experiment longer than 10 seconds induced the considered pair to be rejected. Note that the programs have been written in Java, and were executed on a P300 MMX laptop. Table 1 shows the result of this preliminary experimentation. From this table, it appears that an appropriate selection should be such that: $T_0<0.01$ and *it_max*<100. For our experiments in Section 4.5, we chose the following values: $T_0 = 0.008$, *it_max* = 10, *IT_max* = 100, and $\sigma = 0.99$.

TABLE 1. Selecting Values for T_0 and *it_max*. The CPU Times Are in Milliseconds.

T_0 \ *it_max*	1000	500	250	100	50	10	5	1
0.5	rejected	rejected	rejected	rejected	8199	2544	2100	3079
0.1	rejected	rejected	7585	4473	2764	1957	2124	1478
0.05	rejected	6937	5321	3404	2429	1393	1629	2384
0.01	7290	4053	2222	1880	1828	2412	1066	1771
0.008	7290	3695	2278	2757	1674	1257	1889	2188
0.005	7256	4022	2054	2062	1899	2157	2119	1844
0.003	7276	3674	2575	1704	1264	1826	1440	1453
0.001	7249	4037	2847	1775	1997	2184	2253	1594
0.0005	7941	4836	2353	1695	1910	1510	2448	1072

4.5. Results

We applied the RMA to the 15 representative cross sections shown in Fig. 4(a). Table 2 shows the evolution of Q and *PA* ("Percentage Agreement") for each section. From this table, we can see that Q and *PA* always increased, never decreased. Q rose up to 1.0, and *PA* up to 37.94%. Tables 3 and 4 show the confusion matrices between the control partition and the initial partition, and between the control partition and the final partition, considering all the pixels in the different sections. Thanks to the RMA, the percentage agreement *PA* rose from 73.07% to 87.64%. When considering the classes "reef flat" and "spillway" only, it rose from 50.72% to 81.64%.

Fig. 5 to Fig. 10 show detailed results on the test section, and on sections 1, 3, 5, 7 and 8. In these figures, correct reassignments performed by the RMA are highlighted in cream, incorrect reassignments are highlighted in pink, and desired and however impossible reassignments (because of the strong and wrong opinion expressed by the fuzzy partition) in light gray. The majority of the pixels "spillway" ("reef flat") initially misclassified "reef flat" ("spillway") were correctly reassigned by the RMA: 14th to 17th pixels in the test section (Fig. 5), 13th to 22nd in section 1 (Fig. 6), 30th in section 3 (Fig. 7), 16th to 17th, 20th to 23rd and 26th to 32nd in section 5 (Fig. 8), 15th, 17th to 19th, 21st to 24th, and 28th in section 8 (Fig. 10). The last figure, Fig. 11, shows the results on sections 4-1 to 4-7, which are adjacent. We can see that all of the 17th to 25th initially misclassified pixels were correctly reassigned. Although some of the 26th to 33rd pixels were changed for worse, the classification of this 42×7 extracted image was globally improved (initial *PA* 72.95%, final *PA* 87.92%).

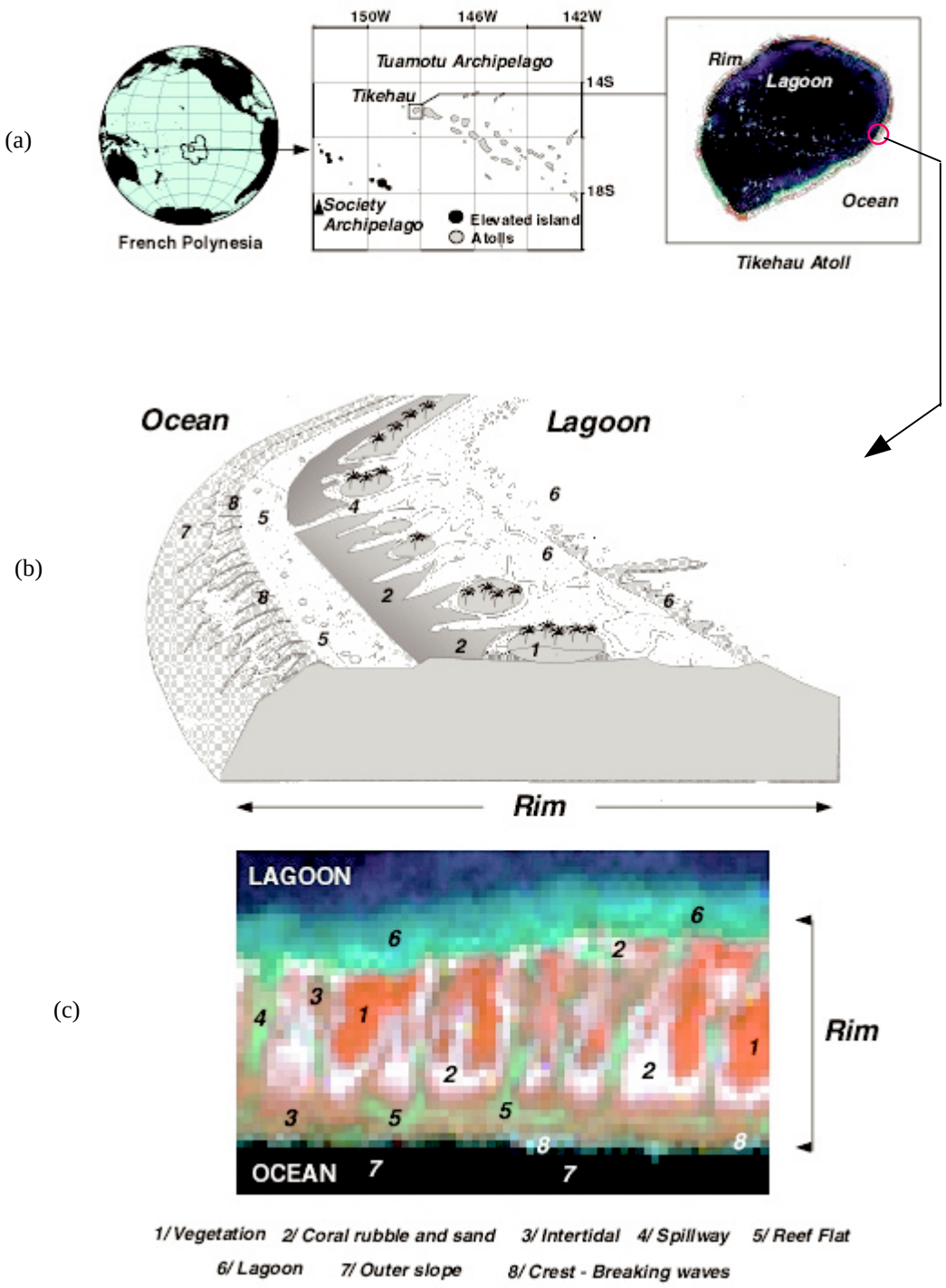

Fig. 2. Tikehau atoll and classes. (a) Location of Tikehau atoll. (b) Location, inside a typical portion of atoll rim (bloc diagram from [23]), of the 8 classes considered in this paper. (c) The classes are readily visible on a Landsat 7 image of the rim.

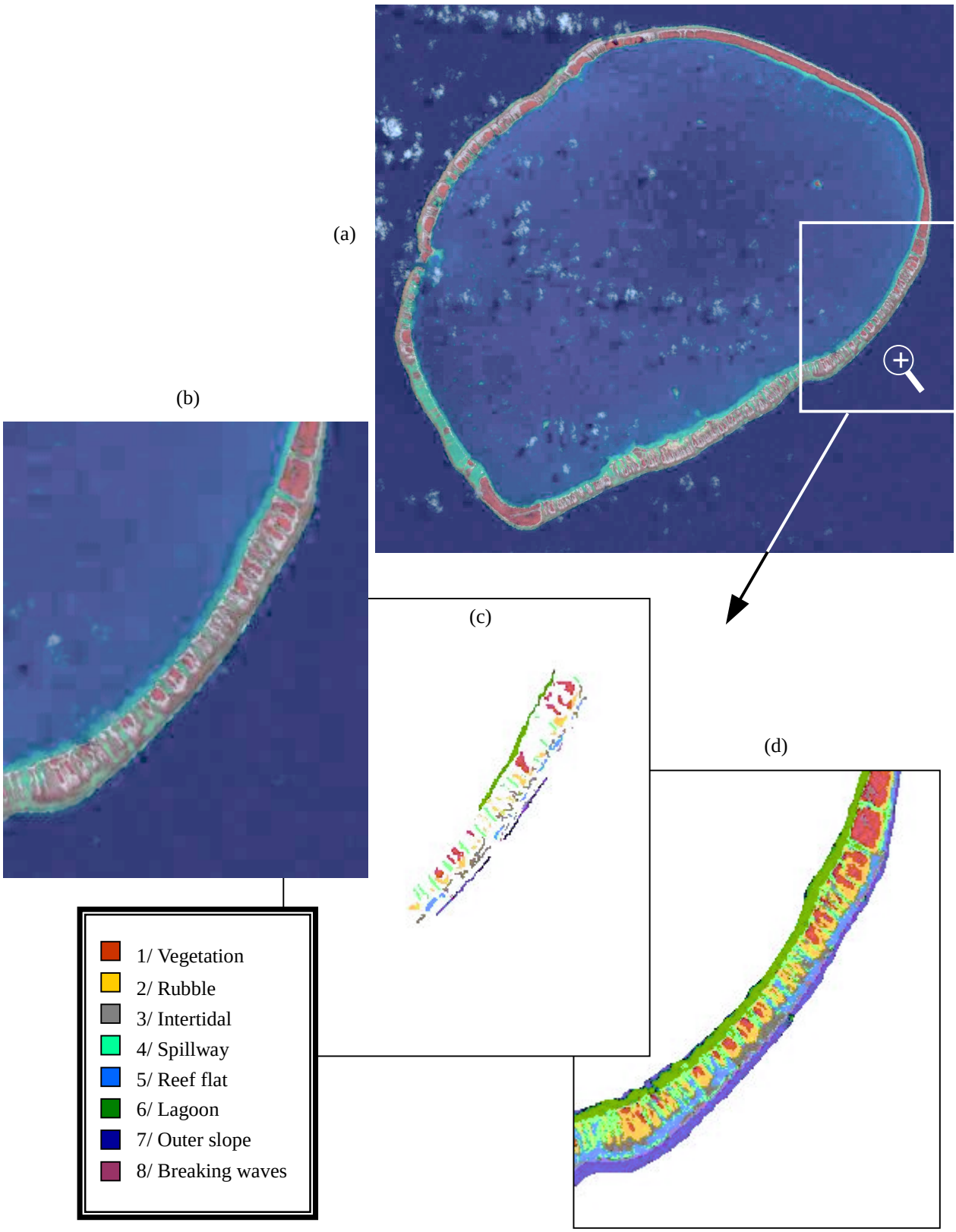

Fig. 3. Landsat 7 image and classification. (a) Landsat 7 image of Tikehau atoll. (b) The studied portion. (c) Training pixels. (d) Result of the supervised classification. The lagoon and the ocean were masked (in white).

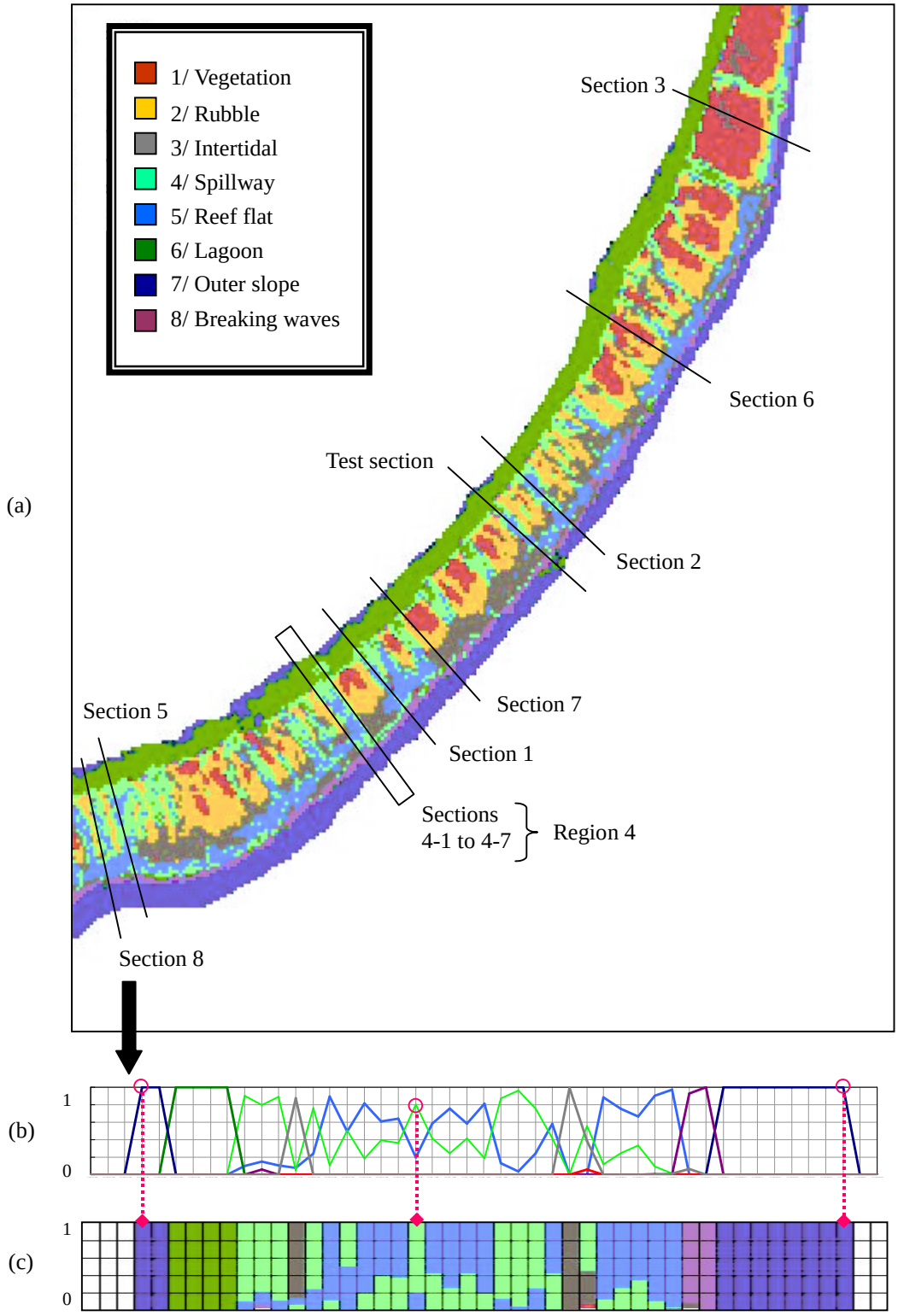

Fig. 4. Partitions and cross sections. (a) Initial 2D crisp partition, and location of the sections considered. (b) 1D fuzzy partition at section 8. (c) Cumulative bar graph representation of (b).

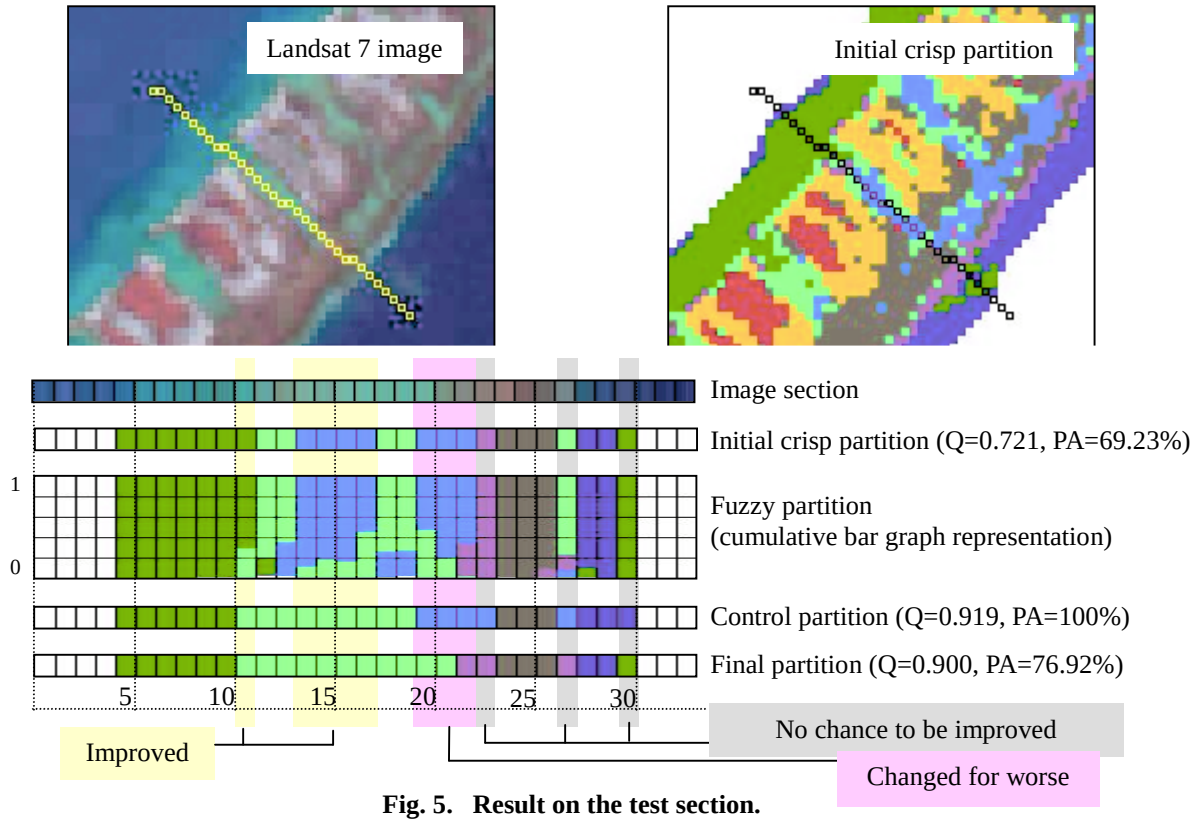

Fig. 5. Result on the test section.

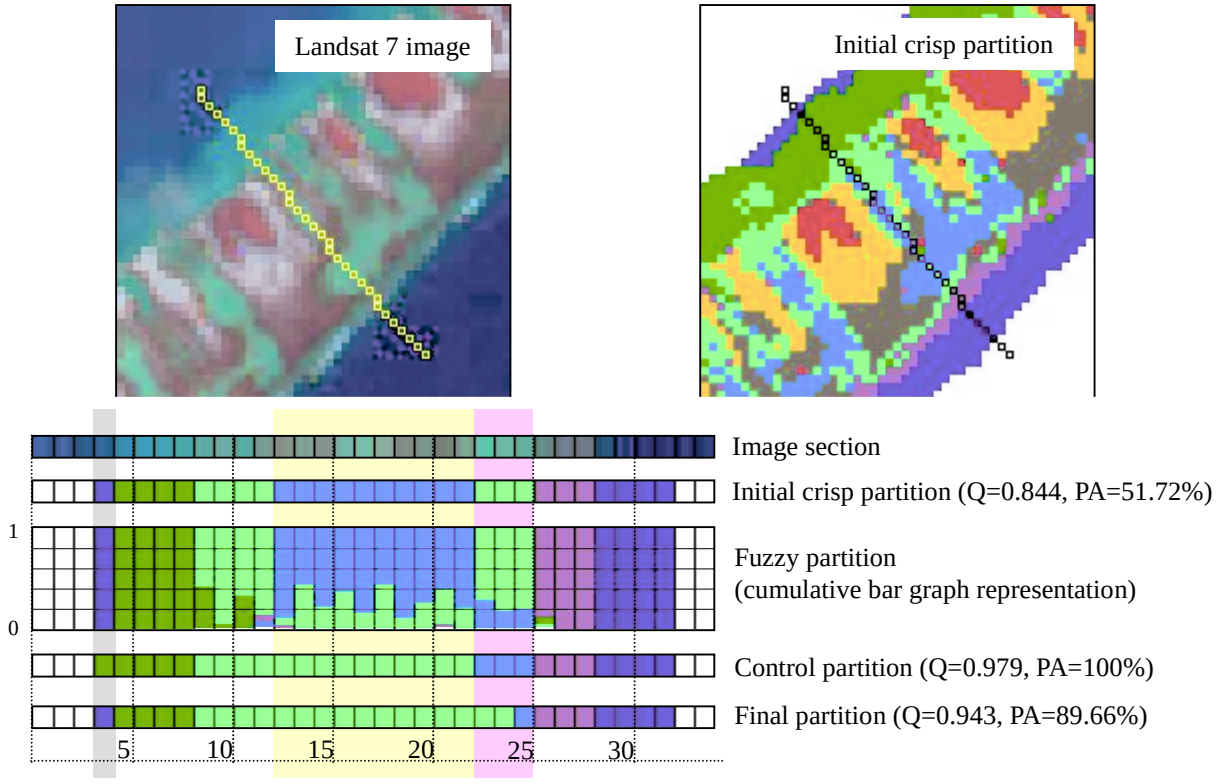

Fig. 6. Result on section 1.

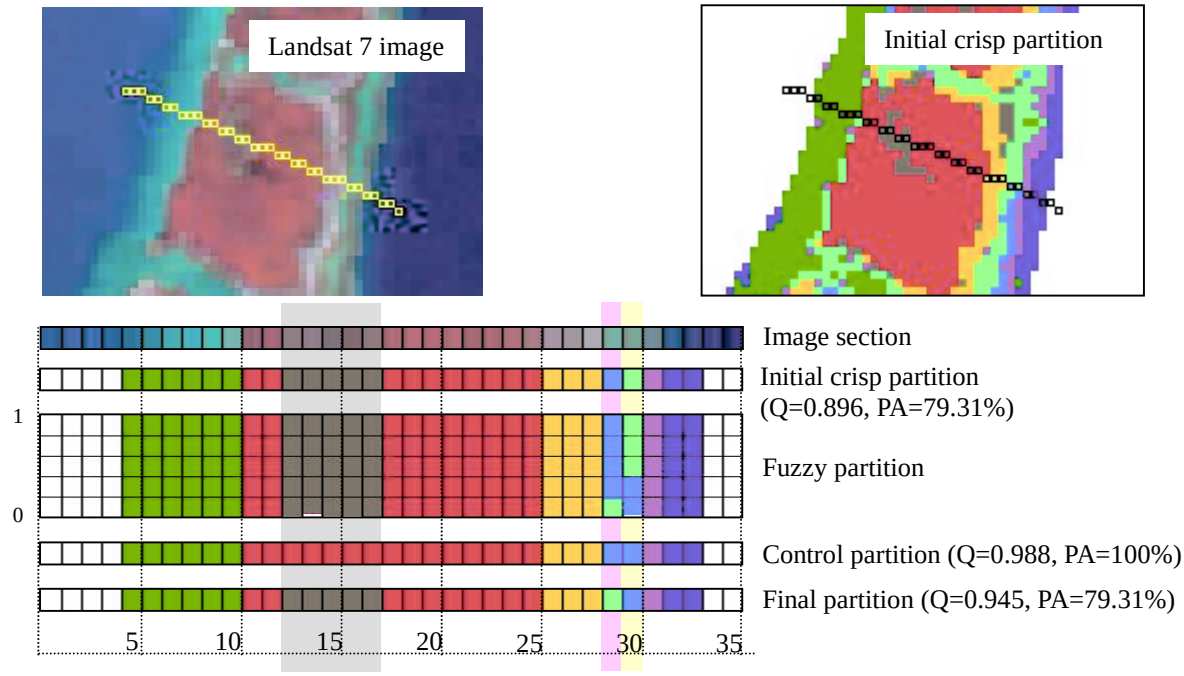

Fig. 7. Result on section 3.

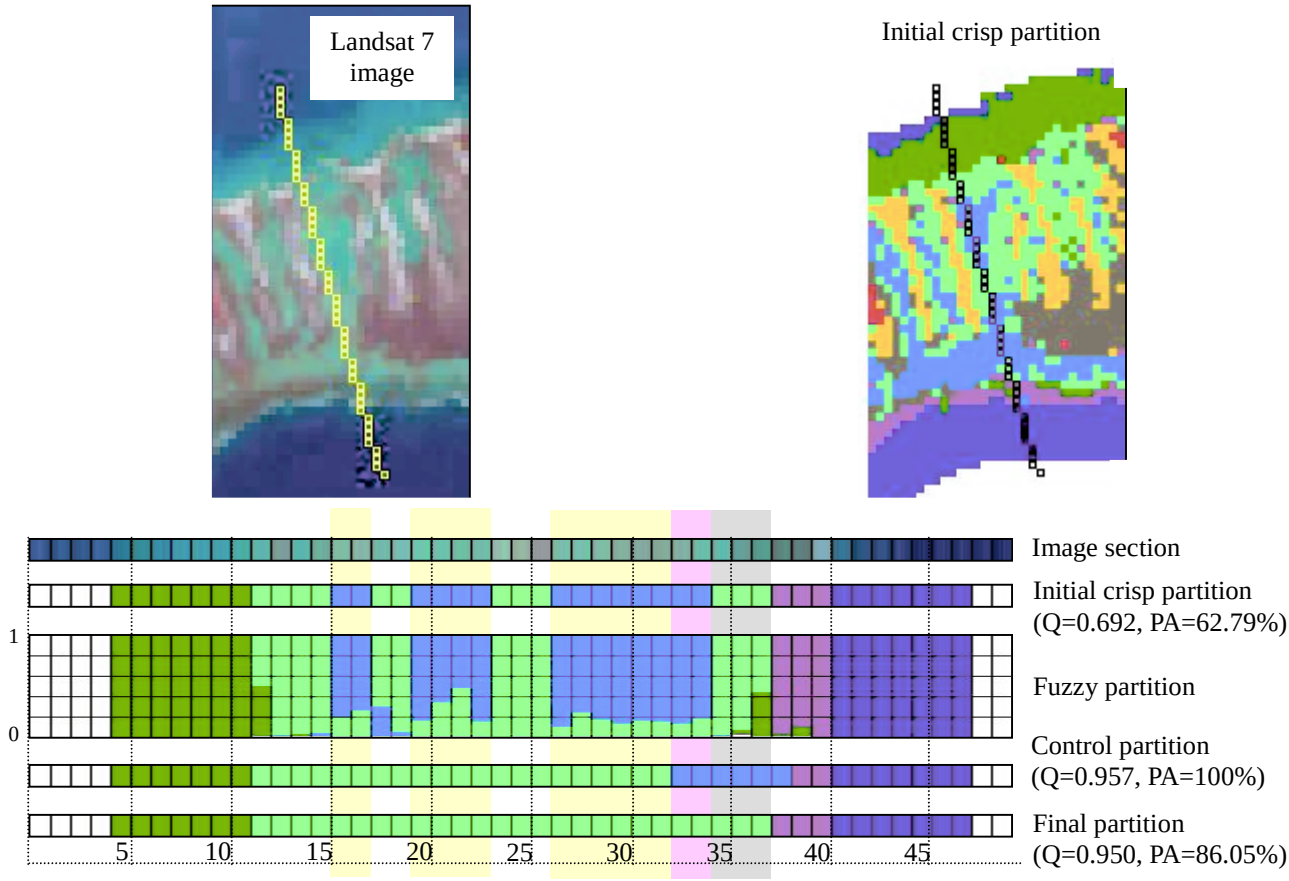

Fig. 8. Result on section 5.

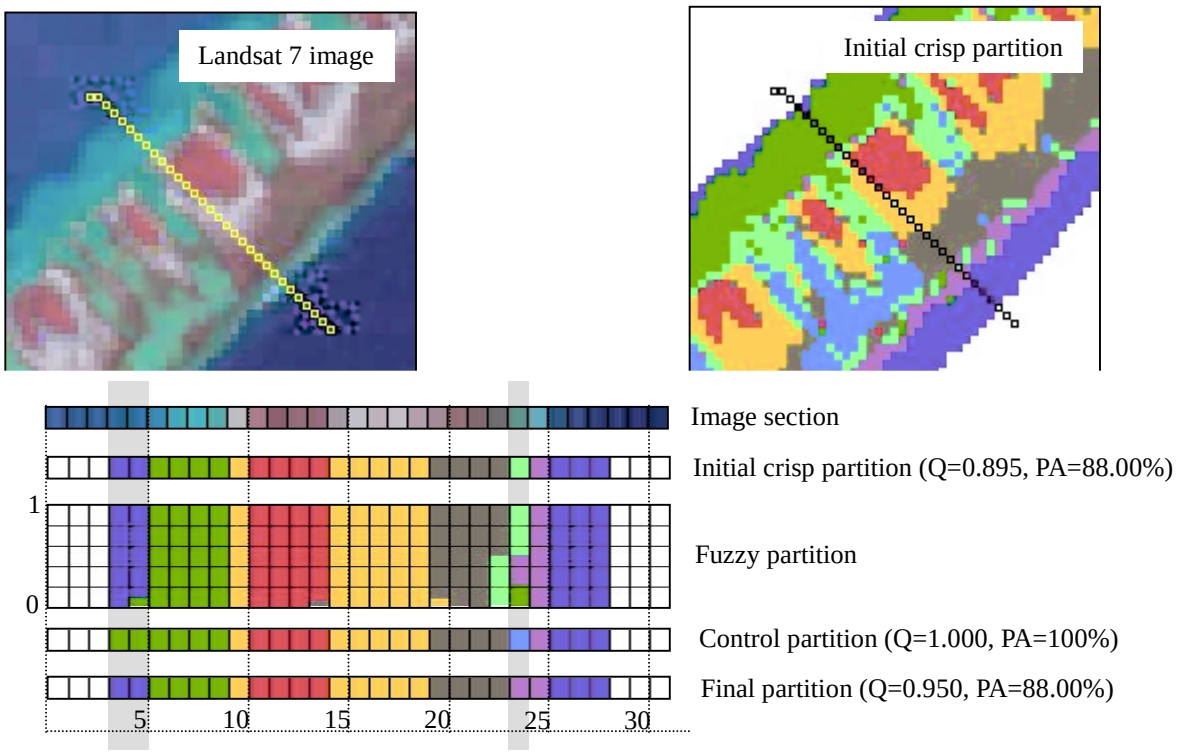

Fig. 9. Result on section 7.

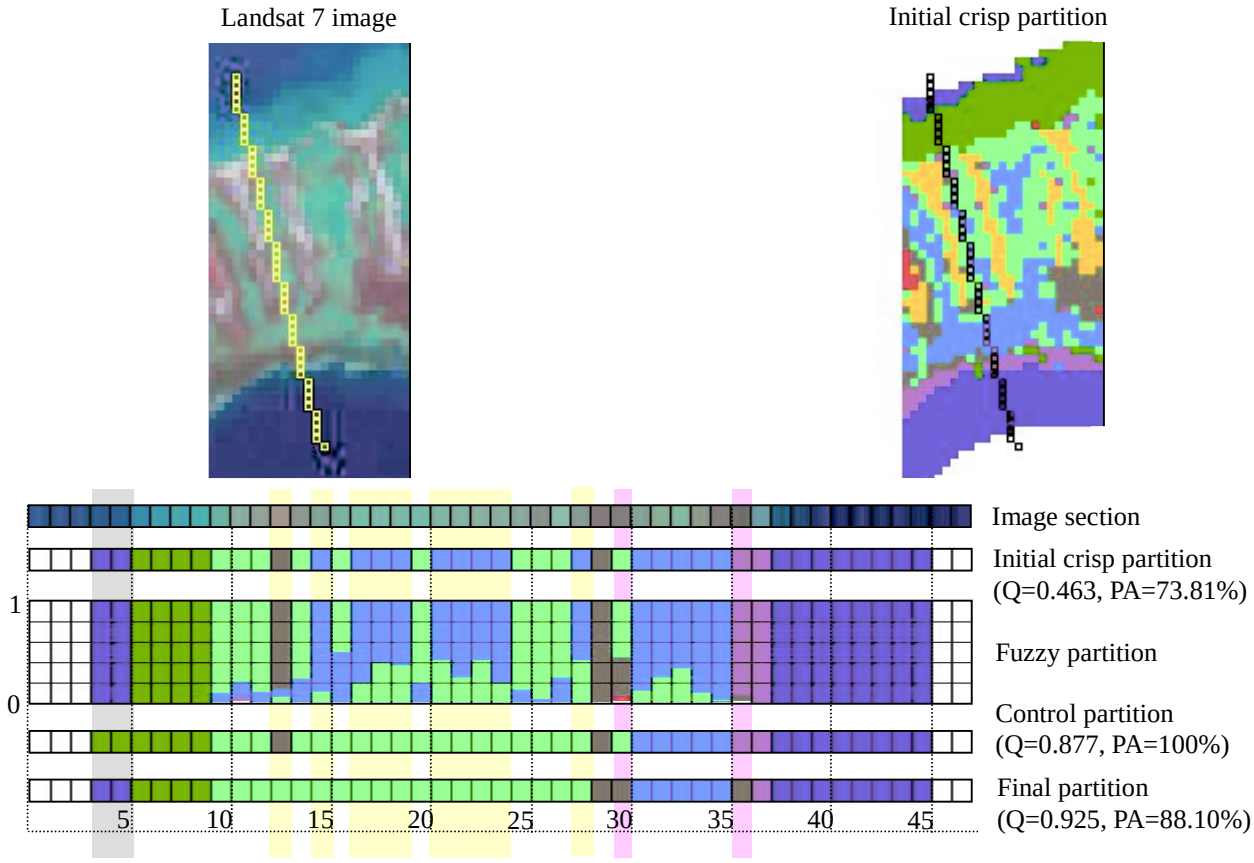

Fig. 10. Result on section 8.

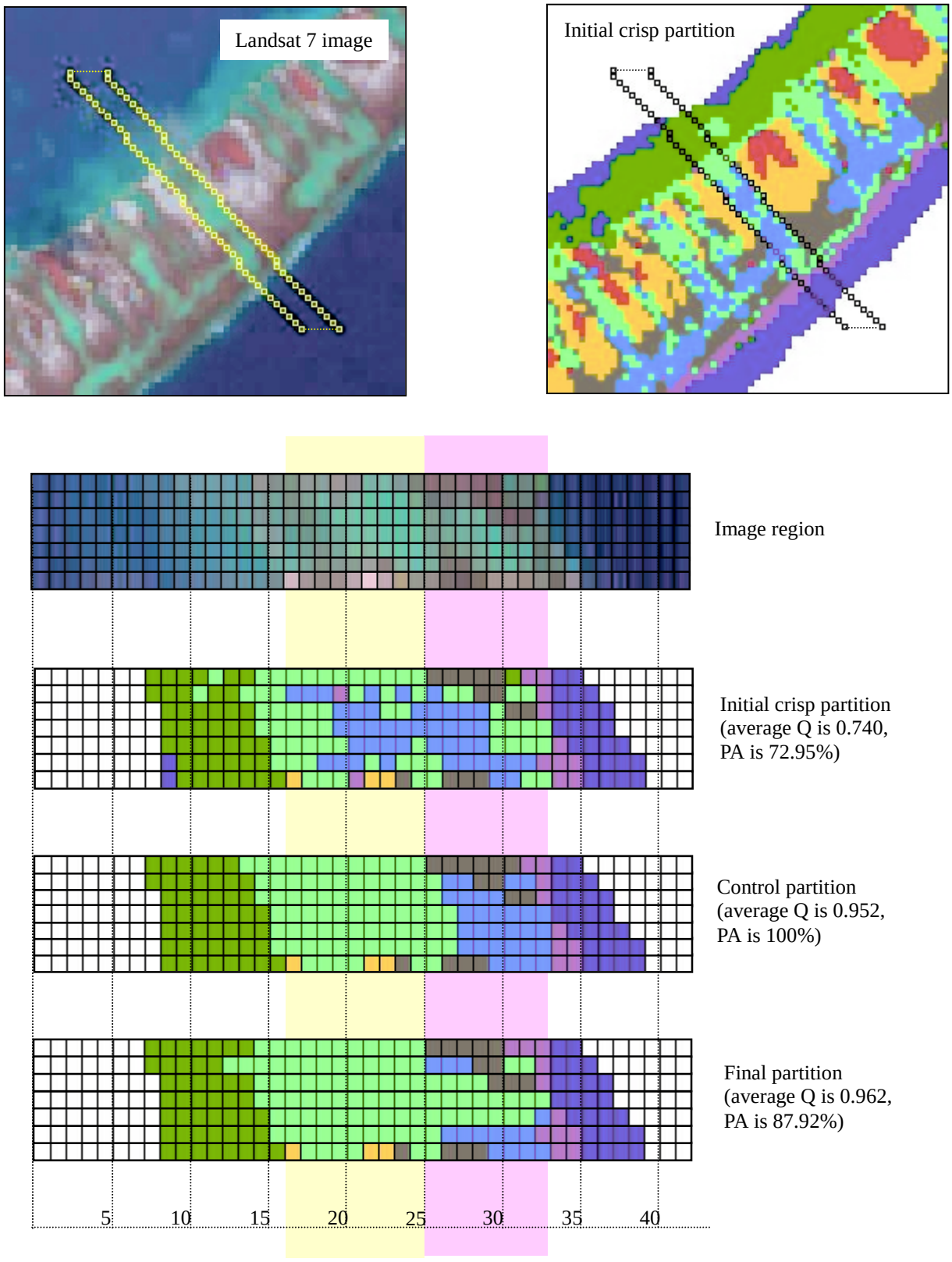

Fig. 11. Result on region 4.

TABLE 2. Evolution of *Q* and *PA* for Each Section

Section	Control Q	Initial Q	Final Q	Initial PA	Final PA	**Improvement**
test	0.919	0.721	0.9	69.23%	76.92%	**+7.69%**
1	0.979	0.844	0.943	51.72%	89.66%	**+37.94%**
2	0.941	0.775	0.945	75%	95.83%	**+20.83%**
3	0.988	0.896	0.945	79.31%	79.31%	**+0%**
4-1	1	0.85	1	89.29%	92.86%	**+3.57%**
4-2	0.928	0.434	0.933	55.17%	82.76%	**+27.59%**
4-3	0.975	0.814	1	79.31%	86.21%	**+6.9%**
4-4	0.95	0.819	0.95	55.17%	75.86%	**+20.69%**
4-5	0.957	0.81	0.993	66.67%	83.33%	**+16.66%**
4-6	0.957	0.708	0.957	77.42%	93.55%	**+16.13%**
4-7	0.9	0.743	0.9	87.1%	100%	**+12.9%**
5	0.957	0.692	0.95	62.79%	86.05%	**+23.26%**
6	1	0.846	0.95	92.86%	96.43%	**+3.57%**
7	1	0.895	0.95	88%	88%	**+0%**
8	0.877	0.463	0.925	73.81%	88.1%	**+14.29%**

TABLE 3. Initial Partition versus Control Partition

In the confusion matrix below, the only pixels considered are the 453 pixels that belong to some section (test section, and sections 1 to 8). *N* denotes the number of control pixels for each class. ***PA* is 73.07%.** Note that *PA* for class 4 only is 50.66%, *PA* for class 5 only is 50.91%, and *PA* for both classes is 50.72%.

class	1	2	3	4	5	6	7	8	total
1	**24**	0	0	0	0	0	0	0	24
2	0	**15**	0	0	0	0	0	0	15
3	5	0	**28**	0	0	0	0	0	33
4	0	0	0	**77**	24	4	0	0	105
5	1	0	0	70	**28**	0	0	0	99
6	0	0	1	2	0	**84**	1	0	88
7	0	0	0	0	0	7	**55**	0	62
8	1	0	0	3	3	0	0	**20**	27
N	31	15	29	152	55	95	56	20	**453**

TABLE 4. Final Partition versus Control Partition

In the confusion matrix below, the only pixels considered are the 453 pixels that belong to some section (test section, and sections 1 to 8). *N* denotes the number of control pixels for each class. ***PA* is 87.64%.** *PA* for class 4 only is 97.37%, *PA* for class 5 only is 38.18%, and *PA* for both classes is 81.64%.

class	1	2	3	4	5	6	7	8	total
1	**25**	0	0	0	0	0	0	0	25
2	0	**15**	0	0	0	0	0	0	15
3	5	0	**27**	1	2	0	0	1	36
4	0	0	1	**148**	26	3	0	0	178
5	0	0	0	2	**21**	0	0	0	23
6	0	0	0	1	0	**87**	1	0	89
7	0	0	0	0	0	5	**55**	0	60
8	1	0	1	0	6	0	0	**19**	27
N	31	15	29	152	55	95	56	20	**453**

Naturally, some pixels were not correctly reassigned by the RMA. Let us discuss some incorrect reassignments. In general, “vegetation” and “rubble” are correctly preclassified. However in section 3, “intertidal” pixels appear in the center of a region “vegetation” with very high membership values (see pixels 13^{th} to 17^{th}, Fig. 7). These pixels have no (or very little) chance to be correctly reassigned by the RMA. For the same reason, several pixels “lagoon” and “outer slope” were not reassigned: 30^{th} pixel in the test section (Fig. 5), 4^{th} in section 1 (Fig. 6), 4^{th} to 5^{th} in section 7 (Fig. 9), and 4^{th} to 5^{th} in section 8 (Fig. 10). Another reason for incorrect decisions is that the RMA *always* accepts a modification of the partition when $Q(X^{cand})$ is equal to or higher than $Q(X^{now})$. As a result, to get a higher Q, correctly classified pixels in the initial crisp partition may be changed for worse. For instance, in section 8 (Fig. 10), the 30^{th} pixel correctly assigned to “spillway” in the initial partition was reassigned to “intertidal”, because the sequence ... ⇒ “spillway” ⇒ “intertidal” ⇒ “spillway” ⇒ “reef flat” ⇒ ... that appears in the control partition is not allowed by *Knowledge 1* (note that the Q of the control partition is lower than the Q of the final partition). On the same section, the 36^{th} pixel was changed accidentally, because this modification gave Q the same value. The same situation is observed at the 22^{nd} pixel in the test section (Fig. 5). In section 5, the 35^{th} pixel, initially misclassified “spillway”, had no chance to be reassigned by the RMA. But the 33^{rd} and 34^{th} pixels, initially well assigned to “reef flat”, were reassigned to “spillway”, in order to get a higher Q. The last example we want to speak about concerns the 29^{th} pixel in section 3. It was incorrectly reassigned from “reef flat” to “spillway” because one of the extracted sections (the section parallel to the coast line) was badly oriented.

Finally, the efficiency of the Region Modification Approach depends on many factors. In particular, the quality of the fuzzy partition (and it would be worth considering using fuzzy possibilistic partitions, as in [26]), the quality of the structural knowledge and the quality of its representation are most important.

5. Conclusion

In this paper, we have described a novel approach that aims at improving the automatic classification of remote sensing images by exploiting expert structural knowledge. It is based on the computation of a fuzzy partition, and the use of a combinatorial optimization strategy.

We have presented first experiments on remote sensing data, a Landsat 7 multispectral image of Tikehau atoll in French Polynesia. Fifteen representative cross sections of the atoll rim were considered. A "one-dimensional" fuzzy partition, extracted from the partition produced by a supervised fuzzy classifier, was associated with each cross section. Our region modification approach was applied to the fifteen 1D partitions by introducing expert structural knowledge concerning the general order of the eight geomorphological classes along the cross sections, and spatial relations on perpendicular sections. The results are very satisfying. For each cross section, the 1D crisp partition attached to the 1D fuzzy partition was modified coherently by appropriately reassigning initially misclassified pixels. The whole image can conceivably be processed in that way.

Much work still has to be done. First, we naturally intend to go one step farther and directly handle 2D regions (instead of 1D sections). Also, we are aware that many factors can affect the results (e.g., the quality of the fuzzy partition, the quality of the knowledge, the way to represent that knowledge and to evaluate its adequacy with image regions). Finally, the computational time is a practical issue that cannot be ignored. Remote sensing images often contain millions of pixels. For instance, how to choose the threshold that is used to select candidate classes? The lower the threshold, the lower the computational time, but the less significant the potential improvement over the initial crisp partition. Which value constitutes a good compromise? We intend to introduce a dynamic threshold controlled with a decreasing function of the number of iterations. We also intend to integrate contextual information into the pixel reassignment process. At the moment, only one pixel differentiates a candidate partition from its parent partition. Many pixels could be simultaneously reassigned, especially neighbors with similar membership values.

Acknowledgment

The authors wish to thank D. Dubois and H. Prade for their precious advice and comments.

References

[1] J. A. Richards, D. A. Landgrebe, and P. H. Swain, "A means for utilizing ancillary information in multispectral classification," *Remote Sensing of Environment*, no. 12, pp. 463-477, 1982.

[2] F. Russo, and G. Ramponi, "Fuzzy methods for multisensor data fusion," *IEEE Trans. Instrumentation and Measurement*, vol. 43, no. 2, pp. 288-294, 1994.

[3] P. Clark, C. Feng, S. Matwin, and K. Fung, "Improving image classification by combining statistical, case-based and model-based prediction methods," *Fundamenta Informatica*, vol. 30, no. 3-4, pp. 227-240, 1996.

[4] G. Shafer, *A mathematical theory of evidence*, Princeton University Press, Princeton, NJ, 1976.

[5] L. A. Zadeh, "Fuzzy sets," *Information and Control*, no. 8, pp. 338-353, 1965.

[6] E. H. Zahzah, and J. Desachy, "Numeric and symbolic data combination for satellite image interpretation," *IGARRS'93 (Int. Geoscience and Remote Sensing Symposium)*, Tokyo, Japan, *Proc.*, pp. 1704-1706, 1993.

[7] L. Tong, J. A. Richards, and P. H. Swain, "Probabilistic and evidential approaches for multisource data analysis," *IEEE Trans. Geosci. Remote Sensing*, vol. 25, pp. 283-293, 1987.

[8] I. Bloch, "Information combination operators for data fusion: A comparative review with classification," *Image and Signal Processing for Remote Sensing*, *Proc. SPIE*, J. Desachy, Ed., vol. 2315, pp. 148-159, 1994.

[9] C. M. Guney, and J. R. G. Townsend, "The use of contextual information in the classification of remotely sensed data," *Photogram. Eng. Remote Sensing*, no. 49, pp. 55-64, 1983.

[10] A. Rosenfeld, R. A. Hummel, and S. W. Zucker, "Scene labeling by relaxation operations," *IEEE Trans. Syst. Man Cybern.*, vol. SMC-6, pp. 420-433, 1976.

[11] P. H. Swain, S. B. Vardeman, and J. C. Tilton, "Contextual classification of multispectral image data," *Pattern Recognition*, vol. 13, no. 6, pp. 429-441, 1981.

[12] B. Solaiman, L. E. Leland, and F. T. Ulaby, "Multisensor data fusion using fuzzy concepts: application to land-cover classification using ERS-1/JERS-1 SAR composites," *IEEE Trans. Geosci. Remote Sensing*, vol. 37, no. 3, pp. 1316-1326, 1999.

[13] E. Binaghi, P. Madella, M.G. Montesano, and A. Rampini, "Fuzzy contextual classification of multisource remote sensing images," *IEEE Trans. Geosci. Remote Sensing*, vol. 35, no. 2, pp. 326-339, 1997.

[14] K. Johnsson, and J. Kanonier, "Knowledge based land-use classification," *IGARRS'91 (Int. Geoscience and Remote Sensing Symposium)*, Helsinki, Finland, *Proc.*, pp. 1847-1850, 1991.

[15] I. B. Türksen, "Measurement of membership functions and their acquisition," *Fuzzy Sets and Systems*, vol. 40, no. 1, pp. 5-38, 1991.

[16] A. Rosenfeld, "The fuzzy geometry of image subsets," *Pattern Recognition Letters*, vol. 2, no. 5, pp. 311-17, 1984.

[17] M. Bao, "Classification of multi-temporal SAR images and INSAR coherence images using adaptive neighborhood model and simulated annealing approach," *20th Asian Conference for Remote Sensing*, Hong Kong, China, *Proc.*, 1999.

[18] K. S. Al-Sultan, "A tabu search approach to the clustering problem," *Pattern Recognition*, vol. 28, no. 9, pp. 1443-1451, 1995.

[19] M. Sonka, S. K. Tadikonda, and S. M. Collins, "Knowledge-based interpretation of MR brain images," *IEEE Trans. Med. Imag.*, vol. 15, no. 4, pp. 443-452, 1996.

[20] H. Suzuki, P. Matsakis, and J. Desachy, "Exploitation de connaissances structurelles en classification d'images : utilisation de méthodes heuristiques d'optimisation combinatoire," *ORASIS 2001 (French-Speaking Conf. on Computer Vision)*, Cahors, France, *Proc.*, pp. 455-464, 2001.

[21] R. Krishnapuram, and J. M. Keller, "A possibilistic approach to clustering," *IEEE Trans. Fuzzy Systems*, vol. 1, no. 2, pp. 98-110, 1993.

[22] R. Battistini *et al.*, "Eléments de terminologie récifale indopacifique," *Thétys*, vol.7, pp. 1-111, 1975.

[23] H. Suzuki, P. Matsakis, and J. Desachy, "Fuzzy Image Classification and Combinatorial Optimization Strategies for Exploiting Structural Knowledge," *FUZZ-IEEE 2001* (*10th IEEE Int. Conf. on Fuzzy Systems*), submitted.

[24] J. C. Bezdek, *Pattern Recognition with Fuzzy Objective Function Algorithms*, Plenum Press, New York, 1981.

[25] I. Gath, and A. B. Geva, "Unsupervised optimal fuzzy clustering," *IEEE Trans. PAMI* , vol. 11 pp. 773-781, 1989.

[26] P. Matsakis, S. Andréfouët, and P. Capolsini, "Evaluation of Fuzzy Partitions," *Remote Sensing of Environment*, vol. 74, no. 3, pp. 515-532, 2000.

[27] S. Andréfouët, M. Claereboudt, P. Matsakis, J. Pagès, and P. Dufour, "Typology of atoll rims in Tuamotu Archipelago (French Polynesia) at landscape scale using SPOT HRV images," *Int. J. Remote Sensing*, vol. 22, no. 6, pp. 987-1004, 2001.

[28] P. Dufour, S. Andréfouët, L. Charpy, and N. Garcia, "Atoll morphometry control nutrient regimes in their lagoons," *Limnology Oceanography*, vol. 46, no. 2, pp. 456-461, 2001.

[29] M. Crochemore, and T. Lecroq, *The Computer Science and Engineering Handbook*, pp. 162-202, CRC Press Inc., Boca Raton, FL, 1996.

[30] V. I. Levenshtein, "Binary codes capable of correcting deletions, insertions and reversals," *Sov. Phys. Dokl.*, vol. 6, pp. 707-710, 1966.